fractal and fractional

MDPI

Article

Microstructure of Epoxy-Based Composites: Fractal Nature Analysis †

Ivana Stajcic [1,*], Aleksandar Stajcic [2], Cristina Serpa [3,4], Dana Vasiljevic-Radovic [2], Branislav Randjelovic [5,6], Vesna Radojevic [7] and Hans Fecht [8,*]

1 Department of Physical Chemistry, "VINČA" Institute of Nuclear Sciences, National Institute of the Republic of Serbia, University of Belgrade, 11351 Belgrade, Serbia
2 Center of Microelectronic Technologies, Institute of Chemistry, Technology, and Metallurgy, National Institute of the Republic of Serbia, University of Belgrade, 11000 Belgrade, Serbia
3 ISEL—Instituto Superior de Engenharia de Lisboa, 1749-016 Lisboa, Portugal
4 CMAFcIO—Centro de Matemática, Aplicações Fundamentais e Investigação Operacional, 1749-016 Lisboa, Portugal
5 Faculty of Electronic Engineering, University of Nis, 18000 Nis, Serbia
6 Teacher Training Faculty, University of Kosovska Mitrovica, 38220 Leposavic, Serbia
7 Faculty of Technology and Metallurgy, University of Belgrade, 11120 Belgrade, Serbia
8 Institute of Functional Nanosystems, University of Ulm, 89077 Ulm, Germany
* Correspondence: ivana_r@vinca.rs (I.S.); hans.fecht@uni-ulm.de (H.F.)
† This paper is the extension of the following research published in The Proceedings of International Conference on Microelectronics-MIEL 2021: Radović, I.M.; Stajčić, A.; Mitić, V.V.; Serpa, C.; Paunović, V.; Ranđelović, B. Fractal reconstruction of fiber-reinforced epoxy microstructure. In Proceedings of the International Conference on Microelectronics, MIEL, Nis, Serbia, 12–14 September 2021; pp. 203–206.

Abstract: Polymers and polymer matrix composites are commonly used materials with applications extending from packaging materials to delicate electronic devices. Epoxy resins and fiber-reinforced epoxy-based composites have been used as adhesives and construction parts. Fractal analysis has been recognized in materials science as a valuable tool for the microstructural characterization of composites by connecting fractal characteristics with composites' functional properties. In this study, fractal reconstructions of different microstructural shapes in an epoxy-based composite were performed on field emission scanning electron microscopy (FESEM) images. These images were of glass fiber reinforced epoxy as well as a hybrid composite containing both glass and electrospun polystyrene fibers in an epoxy matrix. Fractal reconstruction enables the identification of self-similarity in the fractal structure, which represents a novelty in analyzing the fractal properties of materials. *Fractal Real Finder* software, based on the mathematical affine fractal regression model, was employed to reconstruct different microstructure shapes and calculate fractal dimensions to develop a method of predicting the optimal structure–property relations in composite materials in the future.

Keywords: fractal reconstruction; epoxy composites; fiber reinforcement; FESEM analysis

check for updates

Citation: Stajcic, I.; Stajcic, A.; Serpa, C.; Vasiljevic-Radovic, D.; Randjelovic, B.; Radojevic, V.; Fecht, H. Microstructure of Epoxy-Based Composites: Fractal Nature Analysis. *Fractal Fract.* **2022**, *6*, 741. https://doi.org/10.3390/fractalfract6120741

Academic Editor: Zine El Abiddine Fellah

Received: 26 October 2022
Accepted: 13 December 2022
Published: 15 December 2022

1. Introduction

Combining two or more diverse materials can create a new material with different properties concerning the starting components known as composite material [1–3]. The composite design is created in order to improve mechanical, thermal, chemical, and other characteristics of the starting components. All composites have some of the following features that enable them to be used in a wide field of applications: high strength and stiffness, low density, resistance to corrosion and high temperatures, chemical inertness, and durability [4–9]. Among them, epoxy resins and epoxy-based composites are the most frequently used adhesives in the wood, auto, and electronic industries [10,11].

Reinforcement with fibers created improved impact strength, modulus of elasticity, and toughness of the polymer matrix [12]. Micro- and nanostructure control of modern

polymer composites has widened the fields of their application [13–18]. Fiber-reinforced composites (FRC) have been extensively researched and applied as they have excellent mechanical properties and low weights, especially with the fiber diameter reduced to a nanometer size scale [19–23]. Currently, the application of FRC with a polymer matrix extends from structural components in civil and mechanical engineering to micro- and nanocomponents in electronic devices [5]. However, mechanical stress, strain, or impact can cause damage to the fiber-matrix interface and lead to separation, crack formation, and FRC failure [24,25]. Since they are subjected to load, heat, current, or chemicals, it is essential to have insight into how fiber shape and size influence the fiber–epoxy interface and overall composite endurance [26–29].

Microstructural changes at the fiber-matrix interface can be investigated using fractal nature analysis, which is a mathematical technique that offers the possibility of different shape reconstruction [30]. The fractal nature exists within physical system structures and contact surfaces ranging from microstructures down to the nano-scale level to global bulk and massive shapes. Various studies on porosity investigation using fractal geometry have been reported, mostly in ceramic materials [31,32]. Fractal nature analysis is used for the investigation of contact phenomena establishing grain contact models as it offers structural analysis of ceramics and other materials, description and prediction of the shape of grains and pores, along with relations between structural and electric–dielectric properties [33–38]. It has been proven that a fractal reconstruction of pore size and shape in barium titanate ($BaTiO_3$) and modified nano- $BaTiO_3$ can be connected to different dielectric and ferroelectric properties [39].

Recently, this mathematical tool has been employed to define the properties of composite materials [40]. Fractal analysis has been used for microtexture characterization of indium tin oxide/titanium dioxide and silver/diamond-like carbon nanocomposite surfaces obtained with atomic force microscopy (AFM) [41,42]. The influence of the Cu content on structural changes in Cu2O/Cu composite was described using the fractal dimension change rate [43]. Different fractal analysis methods were applied to predict mechanical properties based on the fractal dimension of the fracture surface of the nanoparticle-reinforced vinyl ester [44]. The fractal dimension of the fracture surface was also connected to the impact strength of wood and plastic composites [45]. The percolation model was proposed to show the influence of the carbon nanotube (CNT) structure on the properties of CNT/polymer nanocomposite [40]. Overall, fractal analysis is gaining much attention in the field of composite materials' characterization with efforts to prepare models for various, primarily mechanical, properties. For instance, some authors adopt the maximum positive and maximum negative deviations between measured and trend values to determine the contraction factors [46]. In other research, the fractal dimension computation is based on the experimental dependencies of material strength and porosity [47]. Recently, the relationship between fractal dimension and mechanical properties based on the formation of different aggregates was presented [48]. Small Angle Neutron and X-ray Scattering were used in the fractal analysis of the nanoaggregate structure in asphaltene [49]. However, these techniques enabled investigation of aggregates, but not separate particles and their interactions with the matrix. It would be of great value to obtain a reconstruction of the reinforcement to correlate and predict composite behavior based on its shape and size. Images obtained using field emission scanning electron microscopy (FESEM) could be a microstructural base for performing fractal analysis.

Leading research regarding fractal structure in the literature is focused on assessing the Hausdorff dimension; sometimes, it recurs to previously evaluated vertical factors, but it does not include a total characteristic of that fractal structure. Fractal reconstruction is done in this study by giving a complete mathematical model with all existing theoretical characteristics. A fundamental measure inherent to fractal objects is the Hausdorff dimension (a fractal dimension), which is estimated by the fractal coefficients (usually called vertical or contraction factors).

This paper represents comprehensive research published in the proceedings of the *International Conference on Microelectronics-MIEL 2021*. Glass fiber-reinforced epoxy composite was used as the model material for microstructure fractal nature analysis. This comprehensive research includes fractal reconstruction of PS fiber shape in hybrid composite glass fiber–epoxy–polystyrene (PS) fibers as well as the ring-like shape formed in the solvent-rich area of glass fiber–epoxy–glass capillaries composite. Fiber-reinforced epoxy composite materials were presented in detail in our previously published research [13,14]. Fractal reconstruction based on the mathematical affine fractal regression model used in this research represents a novel approach to finding fractal structure self-similarity. We have shown how the Hausdorff dimension could be used to characterize composite fiber-matrix interface by using this approach on single fibers made from different materials, which is the key to mechanical performance.

2. Materials and Methods

2.1. Materials

Bisphenol A diglycidyl ether epoxy resin-DGEBA was purchased from R&G Faserverbundwerkstoffe GmbH (Composite Technology, Waldenbuch, Germany), as well as hardener based on diethylenetriamine-DETA. The glass fibers were reused material from Izolma (Raca, Serbia). Polystyrene, the first-generation Grubbs catalyst (GC), dimethylformamide 99.8% (DMF), and toluene (TO) were purchased from Sigma-Aldrich (Darmstadt, Germany).

2.2. Processing of Hybrid Composite Materials

2.2.1. Composites with Glass Fibers and Electrospun PS Fibers

Electrospinning (Electrospinner CH-01, Linari Engineering, Pisa, Italy) was performed with the 22 wt % solution of PS in DMF. The procedure was described in detail in our previous research [24]. The setup is presented in Figure 1.

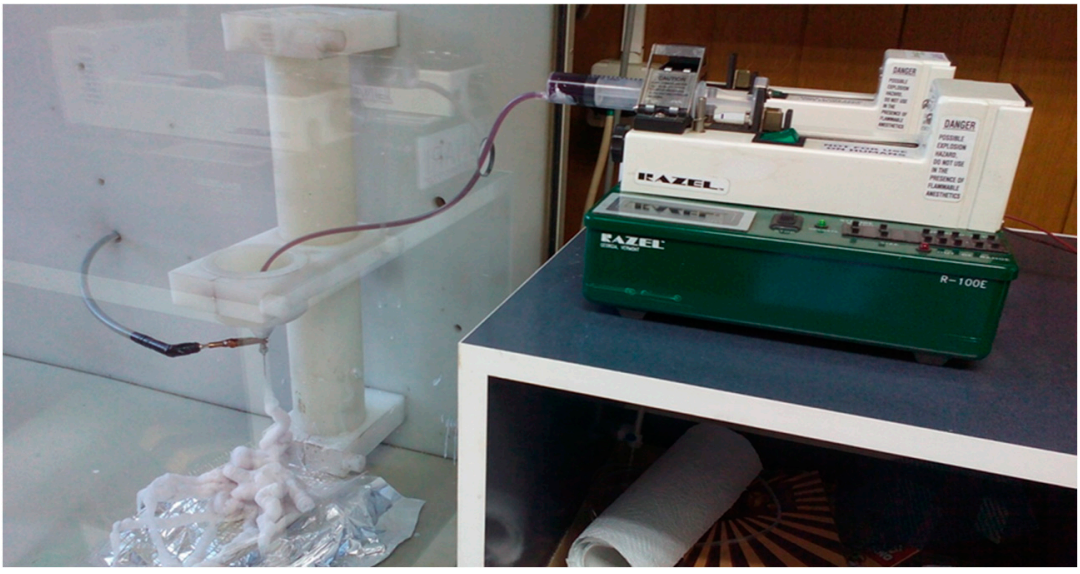

Figure 1. Setup for electrospinning of PS fibers.

DGEBA and DETA were mixed in a 20/9 volumetric ratio and 5.8 wt % of glass fibers were added right after the mixing. The epoxy-based composite was left in a mold for 24 h at room temperature (25 °C). Two types of composites were prepared, including those with and without electrospun PS fibers. The simplified procedure for composite preparation is presented on Scheme 1.

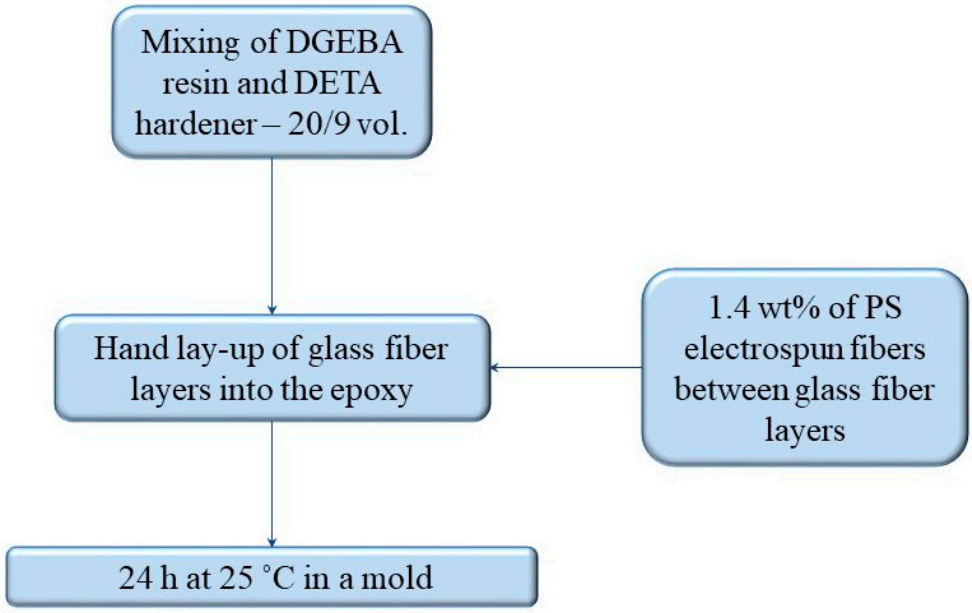

Scheme 1. Preparation of a model composite for fractal analysis.

2.2.2. Composites with Glass Capillaries

Our previous research detailed the preparation of composites with filled glass capillaries [13]. Eight layers of non-woven glass fibers mat were soaked in the epoxy prepared as described in Section 2.2.1. Glass capillaries containing GC/TO and DCPD/DMF mixtures of solutions were placed between the middle glass fiber layers.

2.3. Fractal Shape Reconstruction

Some fractal objects are easily seen as a fractal, but a general object's fractal structure is challenging to see with the naked eye. That is why we need to base our analysis on a precisely defined mathematical function given by Equation (1). The function is defined as self-similar because the image of a part of the domain $\varphi\left(\frac{x+j}{p}\right)$ is obtained as the scaled part of itself $a\varphi(x)$.

Fractal data reconstruction of experimentally determined values is performed using a mathematical *affine fractal regression model* described and explained in the literature [50–52]. The following equation system includes fractal and directional coefficients that should fit experimentally determined and measured values:

$$\varphi\left(\frac{x+j}{p}\right) = a_j\varphi(x) + b_j x + c_j \quad (1)$$

where $x \in [0, 1)$, $0 \leq j \leq p - 1$; a_j stands for fractal coefficients and b_j for directional coefficients, $0 < |a_j| < 1$, with domain [0, 1); and p represents the fractal period. The fractal function φ: $[0, 1) \rightarrow \mathbb{R}$ represents an equation system with a real solution, and its mathematical structure is fractal, i.e., the function's graph is presented as a fractal curve [50,51,53]. Higher fractal oscillations cause increased a_j coefficients. The first fractal level (L) defined by the equations is replicated in the entire domain over all fractal period sub-intervals to build the second fractal level.

A definitive solution to the problem depends on the p-expansion of numbers in domain [0, 1] and is used to find coefficients fitting experimentally measured values. If $L = 2$, the solution is presented through Equations (2)–(4):

$$\varphi(0) = \frac{c_0}{1 - a_0} \quad (2)$$

$$\varphi\left(\frac{\xi_1}{p}\right) = a\xi_1\frac{c_0}{1-a_0} + c\xi_1, \xi_1 \neq 0 \tag{3}$$

$$\varphi\left(\frac{\xi_1}{p} + \frac{\xi_2}{p^2}\right) = a\xi_1\left(a\xi_2\frac{c_0}{1-a_0} + c\xi_2\right) + b\xi_1\frac{\xi_2}{p} + c\xi_1, \xi_2 \neq 0 \tag{4}$$

The sum of square residuals (SSR) is calculated to find optimal coefficients, and its parts are equalized with 0 to minimize the error. Equation (5) must be satisfied to obtain the best problem solution:

$$\frac{\partial SSR}{\partial a_j} = 0, \frac{\partial SSR}{\partial b_j} = 0, \frac{\partial SSR}{\partial c_j} = 0 \tag{5}$$

for all $j = 0, 1, 2, \ldots, p-1$. This represents a 3p parameter problem, which is a nonlinear equation-based estimation.

The analytical solution for this system cannot be applied; therefore, it requires a numerical approach using *Fractal Real Finder* software. Fractal curves and dimensions were estimated using numerical computation where the fractal dimension is a measure of data irregularity. The classical size can be represented by the whole number (integer) in the following manner: 1—lines and curves; 2—two-dimensional objects; 3—three-dimensional objects.

However, some objects have a shape which cannot be described by an integer and require an estimation of a non-integer dimension. The Hausdorff dimension represents a fundamental theoretical mathematical non-integer dimension. A simplified indicator that gives the estimated fractal dimension of experimental data is called a box dimension. The input data are measured values, while the output represents a fractal curve that is the base for fractal dimension estimation [32].

Proposition 1. *The fractal dimension D of the function graph, φ solution of the above system, is upper-bounded by the resolution of the following equation:*

$$\sum_{j=0}^{p-1} {\beta_j}^D = 1 \tag{6}$$

where

$$\beta_j = max\left\{\frac{1}{p}, |a_j|\right\}, 0 \leq p \leq p-1$$

Fractal relevant coefficients are a_j that satisfy $|a_j| > 1/p$.

3. Results and Discussion

Our earlier published research presents a model based on fundamental mathematical theory [30]. Applying the model to actual experimental data requires a procedure to obtain the parameters of a theoretical function or an appropriate fitting method. The commonly used approach is a fractal interpolation which does not result in the complete estimation of all parameters, such as fractal coefficients. This work presents fractal regression resulting in a method that finds all theoretical model parameters that approximately fit actual data, which is a specific case of a theoretical model published earlier [30]. The fractal dimension can be estimated based on the proposed fractal function and the obtained fractal coefficients. FESEM images of two composites were used as materials for the practical application of fractal regression-based data reconstruction. The aim was to reconstruct fiber shapes and find fractal dimensions. The fractal is theoretically characterized by self-similarity which is given by an infinite number of fractal levels and replicates configurations in more minor scales. The standard domain is always given at the interval [0,1), regardless of the original image's scale, and for the range, we provide an interval with one digit for the unities. The scale is given only for authentic images in appropriate units.

3.1. Glass Fiber Shape Reconstruction

The first model composite was the glass fibers–epoxy composite, and surface FESEM images are presented in Figure 2. One glass fiber was selected and enlarged for the purpose of shape reconstruction (Figure 3).

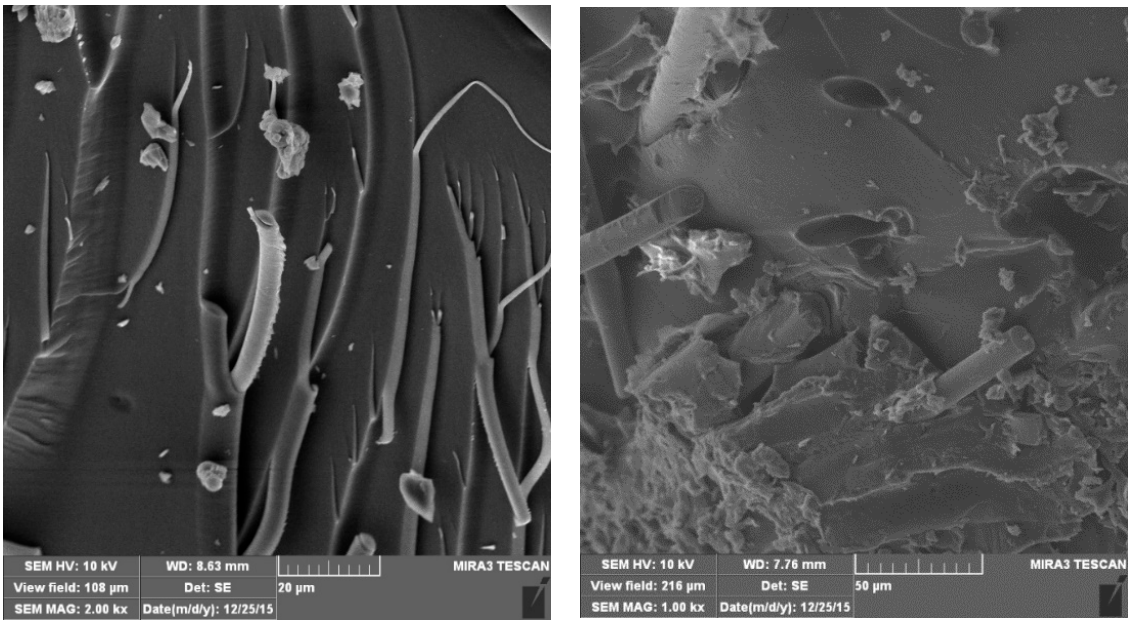

Figure 2. FESEM images of glass fiber–epoxy composite.

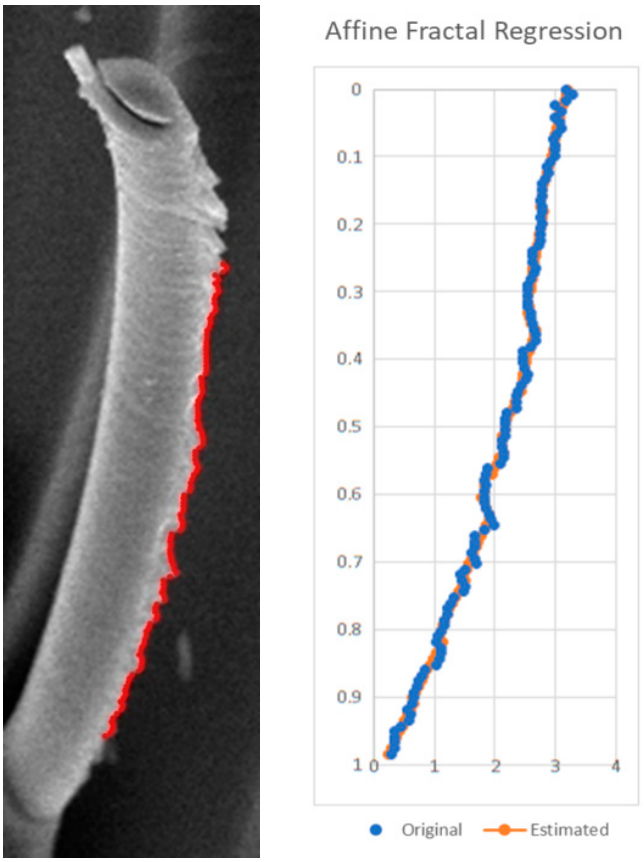

Figure 3. Enlarged glass fiber (**left**) and estimated fractal curve of a fiber (**right**).

The border line was created using red points, and the resulting fractal shape reconstruction is presented in Figure 3 (right). The function domain was set in the vertical axis to adjust to the fiber position. The software evaluation of all possible fractal shapes was performed, as well as fractal reconstruction of the curve with 11 fractal periods ($p = 11$) and 2 fractal levels ($L = 2$). The number of points was calculated using the following equation:

$$p^L = 11^2 = 121 \quad (7)$$

The coefficients of the fractal curve (Figure 3 left) are presented in Table 1.

Table 1. Estimated Coefficients of the Fractal Curve.

	0	**1**	**2**	**3**	**4**	**5**
a_j	−0.058	−0.086	−0.009	−0.229	−0.076	−0.161
b_j	−0.397	−0.47	−0.224	−0.606	−0.446	−0.701
c_j	3.39	3.256	2.849	3.371	2.896	2.886
	6	**7**	**8**	**9**	**10**	
a_j	−0.365	−0.021	−0.097	0.001	−0.017	
b_j	−1.2	−0.518	−0.725	−0.561	−0.54	
c_j	3.244	1.976	1.809	1.135	0.703	

The software obtained a glass fiber Hausdorff dimension of 1.21968, which was calculated using Equation (6) and approximated a regular line shape. This could be applied further to composite processing, leading to an assumption that the processing technique resulted in a regular-shaped fiber.

3.2. Electrospun PS Fiber Shape Reconstruction

The FESEM image of the glass fibers–epoxy–polystyrene hybrid composite surface is presented in Figure 4, from which electrospun polystyrene fiber is enlarged for fractal analysis in Figure 5.

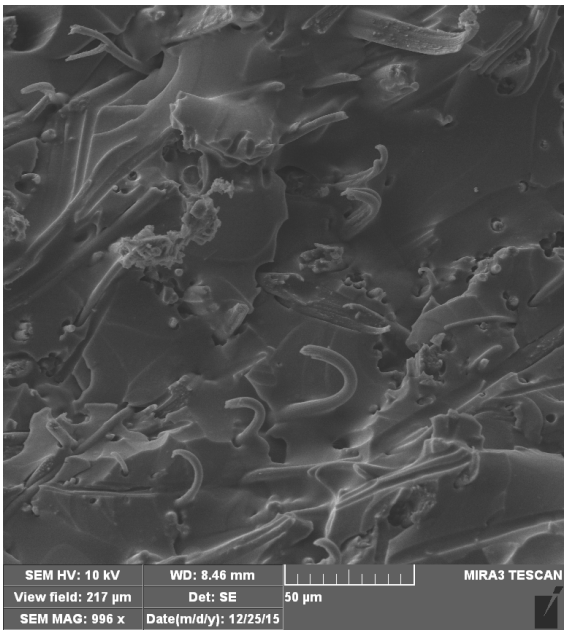

Figure 4. FESEM image of glass fibers–epoxy–PS fibers hybrid composite.

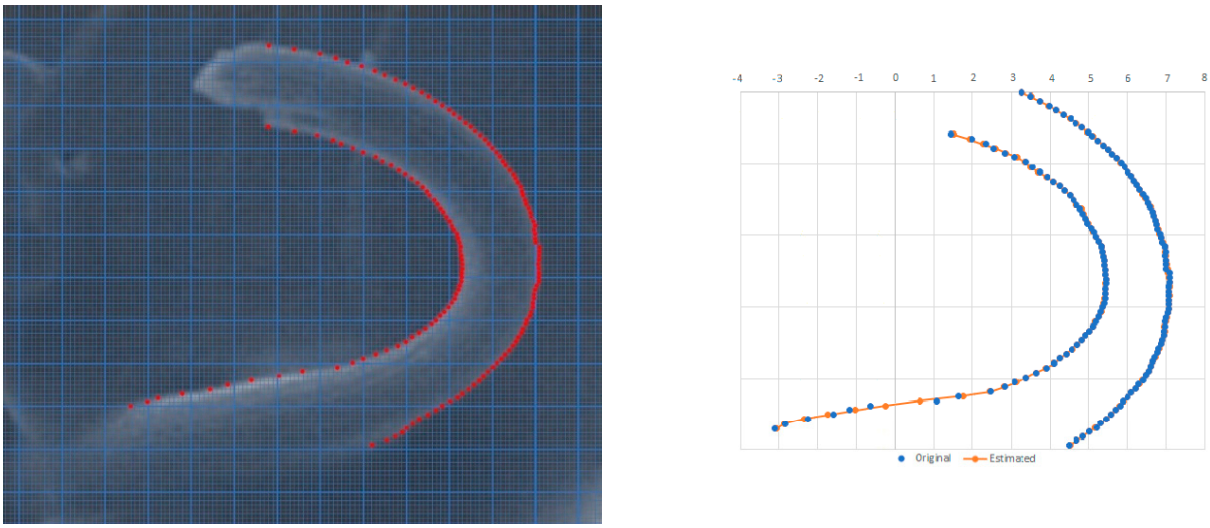

Figure 5. Enlarged polystyrene fiber (**left**) and estimated fractal curves (**right**).

Using the same procedure as in Section 3.1, Fractal Real Finder software was used for the sequences of points and the estimated fractal models with coefficients, as presented in Tables 2 and 3. There were nine fractal periods ($p = 9$) and two fractal levels ($L = 2$) for the left fractal curve, while $p = 8$ and L were the same for the right fractal curve. Following Equation (7), these point sequences had 81 and 64 elements.

Table 2. Estimated Coefficients of the Left Fractal Curve.

	0	**1**	**2**	**3**	**4**	**5**	**6**	**7**
a_j	0.056	0.036	−0.006	0.001	0.017	0.021	0.042	−0.195
b_j	2.197	1.069	0.485	0.113	−0.188	−0.841	−2.021	−5.291
c_j	1.402	3.542	4.711	5.2	5.253	4.999	4.087	1.997

Table 3. Estimated Coefficients of the Right Fractal Curve.

	0	**1**	**2**	**3**	**4**	**5**	**6**	**7**	**8**
a_j	0.047	0.015	0.011	−0.006	0.0	0.019	0.016	0.015	0.027
b_j	1.634	1.026	0.639	0.351	0.14	−0.179	−0.455	−0.898	−1.407
c_j	3.108	4.928	5.963	6.675	6.968	6.998	6.907	6.506	5.601

The estimated fractal curves were very close to the original points. The coefficients of the left curve are presented in Table 2.

The coefficients of the right fractal estimated curve are presented in Table 3.

Both fractal reconstructions revealed no relevant fractal coefficients; consequently, the corresponding Hausdorff dimension estimate was 1, which indicated a highly regular shape of the electrospun PS fiber.

The difference in the Hausdorff dimension between fibers came from the fiber-matrix interaction. Urea-treated glass fibers interacted better with epoxy matrix, which resulted in matrix fracture with epoxy residual on the glass fiber that caused minor shape irregularity. In contrast, PS–epoxy interactions were not that strong, which resulted in fiber-matrix separation that left the fiber surface shape intact. Stronger bonding between the fiber and the matrix led to a higher mechanical strength of the composite material. In this manner, the Hausdorff dimension could give us a practical example of the reinforcement-matrix interface properties and help predict mechanical properties in future experiments.

3.3. Ring-Like Shape Reconstruction

Fractal shape reconstruction was performed on a ring-like structure observed at the fracture site of the glass fiber–epoxy–glass capillaries presented in Figure 6. Enlagred microstructure and fractal curve are presented in Figure 7.

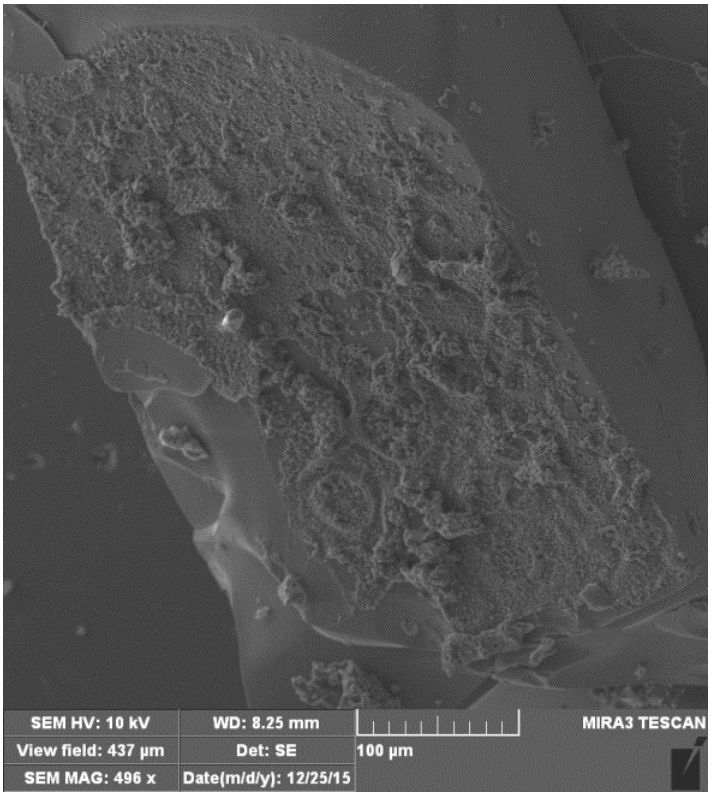

Figure 6. FESEM image of glass fiber–epoxy–glass capillaries composite.

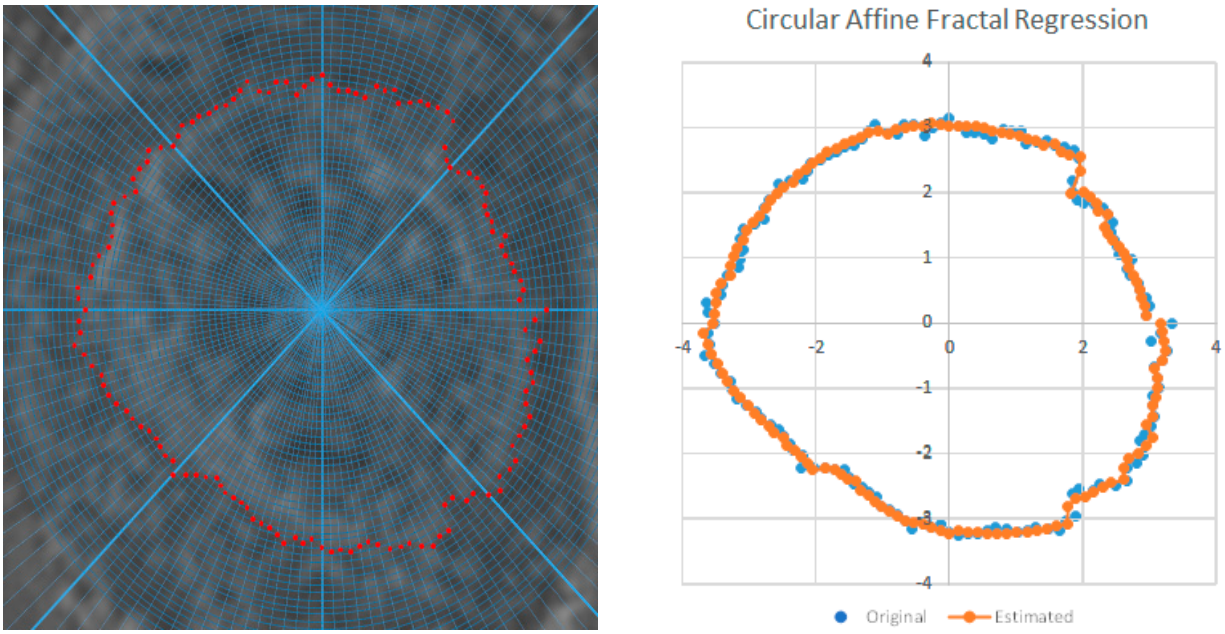

Figure 7. Zoomed image with the red contour points marked and the estimated fractal curve.

Polar coordinates were used to perform the fractal analysis, with $144 = 12^2$ points. These corresponded to the sequence of radius given by the contour. There were 9 fractal periods ($p = 9$) and 2 fractal levels ($L = 2$) for the left fractal curve.

The obtained coefficients are given in Table 4 which apply the same method as the previous images, including 12 fractal periods ($p = 12$) and 2 fractal levels ($L = 2$).

Table 4. Estimated Coefficients of the Fractal Curve from Polar Coordinates.

	0	**1**	**2**	**3**	**4**	**5**
a_j	−0.057	−0.499	−0.051	−0.113	−0.066	−0.139
b_j	−0.195	0.648	−0.048	0.178	0.155	0.308
c_j	3.123	4.226	3.221	3.368	3.363	3.729
	6	**7**	**8**	**9**	**10**	**11**
a_j	0.022	0.196	0.058	−0.029	0.208	−0.168
b_j	−0.62	−0.445	0.335	0.41	0.126	−0.104
c_j	3.63	2.549	2.71	3.253	2.7	3.829

The plot of this fractal fitting is shown in Figure 7.

The results found an estimated Hausdorff dimension of 1.37857. Various phenomena observed through microstructural shapes could be studied using this method, and the results could be applied in processing and properties predictions of materials.

4. Conclusions

This research presents an application of the fractal regression method in the shape reconstruction of fibers in epoxy-based composites, which are commonly used insulators. This method is developed to find all theoretical model parameters that approximately fit the actual data, and it enables the estimation of fractal function and coefficients used to calculate the fractal dimension. Fractal reconstruction is an innovation compared with previous works that analyze the fractal properties of materials. It represents a tool that could help us understand how processing parameters influence the microstructure that dictates mechanical properties. In this study, we presented a fractal function fitting the shape of chosen microstructures. The traditional fractal dimension (or the Hausdorff dimension) estimation gives only a part of the fractal characteristics of the objects of analysis. This new method's advantage is finding the self-similarity in the fractal structure. The glass fiber shape was reconstructed using Fractal Real Finder software, and the resulting fractal dimension of 1.21968 indicates minor shape irregularity. After the calculations, electrospun polystyrene fiber from a glass fiber–epoxy–polystyrene fiber hybrid composite had an estimated fractal dimension of 1, which shows that this processing method resulted in a highly ordered shape. The differences in Hausdorff dimensions between the urea-treated glass and the PS fiber is caused by the stronger interaction of the glass fiber with the epoxy matrix that resulted in epoxy residual on the surface of the fiber. PS fiber and epoxy debonded, which resulted in an intact fiber surface. Fiber-matrix interaction strongly influences mechanical properties of composite material; thus, the Hausdorff dimension could help connect microstructural differences and mechanical performances of composites. The third fractal reconstruction of the microstructural ring-like shape formation after the fracture resulted in a fractal dimension of 1.37857. Fractal shape reconstruction showed that the practical application of fractal regression could help process parameter analysis and the future prediction of optimal composite preparation based on the desired reinforcement-matrix interactions that further enable control of the mechanical properties, which is highly important for the endurance of sensitive and atmosphere-exposed materials.

Author Contributions: Conceptualization, I.S. and A.S.; methodology, I.S.; software, C.S.; validation, I.S., A.S., and D.V.-R.; formal analysis, B.R. and C.S.; investigation, V.R.; writing—original draft preparation, I.S. and A.S.; writing—review and editing, D.V.-R.; visualization, A.S.; funding acquisition, H.F. All authors have read and agreed to the published version of the manuscript.

Funding: This work was financially supported by the Ministry of Education, Science and Technological Development of the Republic of Serbia (Grant No. 451-03-9/2022-14/200017 and 451-03-68/2022-14/200026) and project ESA ThermoLab-ISS/project number AO-2009-1020, and it recieved partial support from the Portuguese National Funding from FCT—Fundação para a Ciência e a Tecnologia under the project: UIDB/04561/2020.

Data Availability Statement: Not applicable.

Conflicts of Interest: The authors declare no conflict of interest. The funders had no role in the design of the study; in the collection, analyses, or interpretation of data; in the writing of the manuscript; or in the decision to publish the results.

References

1. Radović, I.M.; Stajčić, A.; Mitić, V.V.; Serpa, C.; Paunović, V.; Ranđelović, B. Fractal reconstruction of fiber-reinforced epoxy microstructure. In Proceedings of the International Conference on Microelectronics, MIEL, Nis, Serbia, 12–14 September 2021; pp. 203–206.
2. Kaw, A.K. *Mechanics of Composite Materials*, 2nd ed.; CRC Press: Boca Raton, FL, USA, 2006.
3. Callister, W.D., Jr. *Materials Science and Engineering: An Introduction*, 7th ed.; John Wiley & Sons, Inc.: New York, NY, USA, 2007.
4. Zucchelli, A.; Focarete, M.L.; Gualandi, C.; Ramakrishna, S. Electrospun nanofibers for enhancing structural performance of composite materials. *Polym. Adv. Technol.* **2011**, *22*, 339–349. [CrossRef]
5. Zhang, P.; Li, G. Advances in healing-on-demand polymers and polymer composites. *Prog. Polym. Sci.* **2016**, *57*, 32–63. [CrossRef]
6. Bailey, B.M.; Leterrier, Y.; Garcia, S.J.; van der Zwaag, S.; Michaud, V. Electrically conductive self-healing polymer composite coatings. *Prog. Org. Coat.* **2015**, *85*, 189–198. [CrossRef]
7. Chortos, A.; Liu, J.; Bao, Z. Pursuing prosthetic electronic skin. *Nat. Mater.* **2016**, *15*, 937–950. [CrossRef]
8. Murphy, E.B.; Wudl, F. The world of smart healable materials. *Prog. Polym. Sci.* **2010**, *35*, 223–251. [CrossRef]
9. Kou, Y.; Cheng, X.; Macosko, C.W. Degradation and Breakdown of Polymer/Graphene Composites under Strong Electric Field. *J. Compos. Sci.* **2022**, *6*, 139. [CrossRef]
10. Chen, K.; Zhao, X.; Zhang, F.; Wu, X.; Huang, W.; Liu, W.; Wang, X. Influence of gamma irradiation on the molecular dynamics and mechanical properties of epoxy resin. *Polym. Degrad. Stab.* **2019**, *168*, 108940. [CrossRef]
11. Sharma, A.; Jung, D.H.; Cheon, J.S.; Jung, J.P. Epoxy Polymer Solder Pastes for Micro-Electronic Packaging Applications. *J. Weld. Join.* **2019**, *37*, 7–14. [CrossRef]
12. Mallick, P.K. *Fiber-Reinforced Composites: Materials, Manufacturing, and Design*; Taylor & Francis Group, LLC CRC Press: Boca Raton, FL, USA, 2008.
13. Radovic, I.; Stajcic, A.; Radisavljevic, A.; Veljkovic, F.; Cebela, M.; Mitic, V.V.; Radojevic, V. Solvent effects on structural changes in self-healing epoxy composites. *Mater. Chem. Phys.* **2020**, *256*, 123761. [CrossRef]
14. Radovic, I.M.; Stojanovic, D.B.; Kojovic, A.; Petrovic, M.; Uskokovic, P.S.; Radojevic, V.J.; Aleksic, R.R. Healing efficiency of polystyrene electrospun nanofibers with Grubbs catalyst in thermosetting composite. *J. Compos. Mater.* **2017**, *51*, 3003–3016. [CrossRef]
15. Kanu, N.J.; Gupta, E.; Vates, U.K.; Singh, G.K. Self-healing composites: A state-of-the-art review. *Compos. Part A Appl. Sci. Manuf.* **2019**, *121*, 474–486. [CrossRef]
16. Zhang, Q.; Zhao, X.; Sui, G.; Yang, X. Surface Sizing Treated MWCNTs and Its Effect on the Wettability, Interfacial Interaction and Flexural Properties of MWCNT/Epoxy Nanocomposites. *Nanomaterials* **2018**, *8*, 680. [CrossRef] [PubMed]
17. Wang, T.; Song, B.; Wang, L. A New Filler for Epoxy Resin: Study on the Properties of Graphite Carbon Nitride (g-C_3N_4) Reinforced Epoxy Resin Composites. *Polymers* **2020**, *12*, 76. [CrossRef] [PubMed]
18. Awad, S.; Hamouda, T.; Midani, M.; Zhou, Y.; Katsou, E.; Fan, M. Date palm fibre geometry and its effect on the physical and mechanical properties of recycled polyvinyl chloride composite. *Ind. Crops Prod.* **2021**, *175*, 114172. [CrossRef]
19. Ellyin, F.; Maser, R. Environmental effects on the mechanical properties of glass-fiber epoxy composite tubular specimens. *Compos. Sci. Technol.* **2004**, *64*, 1863–1874. [CrossRef]
20. Park, J.S.; Kim, H.S.; Thomas Hahn, H. Healing behavior of a matrix crack on a carbon fiber/mendomer composite. *Compos. Sci. Technol.* **2009**, *69*, 1082–1087. [CrossRef]
21. Peterson, A.M.; Jensen, R.E.; Palmese, G.R. Thermoreversible and remendable glass–polymer interface for fiber-reinforced composites. *Compos. Sci. Technol.* **2011**, *71*, 586–592. [CrossRef]
22. Li, G.; Ajisafe, O.; Meng, H. Effect of strain hardening of shape memory polymer fibers on healing efficiency of thermosetting polymer composites. *Polymer* **2013**, *54*, 920–928. [CrossRef]
23. Patel, A.J.; Sottos, N.R.; Wetzel, E.D.; White, S.R. Autonomic healing of low-velocity impact damage in fiber-reinforced composites. *Comp. Part A* **2010**, *41*, 360–368. [CrossRef]
24. Ghosh, S.K. *Self-Healing Materials: Fundamentals, Design Strategies, and Applications*; Ghosh, S.K., Ed.; WILEY-VCH Verlag GmbH & Co. KGaA: Weinheim, Germany, 2009.
25. Scheiner, M.; Dickens, T.J.; Okoli, O. Progress towards self-healing polymers for composite structural applications. *Polymer* **2016**, *83*, 260–282. [CrossRef]

26. Yin, T.; Rong, M.Z.; Wu, J.; Chen, H.; Zhang, M.Q. Healing of impact damage in woven glass fabric reinforced epoxy composites. *Comp. Part A* **2008**, *39*, 1479–1487. [CrossRef]
27. Wang, C.H.; Sidhu, K.; Yang, T.; Zhang, J.; Shanks, R. Interlayer self-healing and toughening of carbon fibre/epoxy composites using copolymer films. *Comp. Part A* **2012**, *43*, 512–518. [CrossRef]
28. Lee, J.; Bhattacharyya, D.; Zhang, M.Q.; Yuan, Y.C. Mechanical properties of a self-healing fibre reinforced epoxy composites. *Comp. Part B* **2015**, *78*, 515–519. [CrossRef]
29. Huan, S.; Liu, G.; Han, G.; Cheng, W.; Fu, Z.; Wu, Q. Effect of Experimental Parameters on Morphological, Mechanical and Hydrophobic Properties of Electrospun Polystyrene Fibers. *Materials* **2015**, *8*, 2718–2734. [CrossRef]
30. Mitić, V.V.; Lazović, G.; Paunović, V.; Cvetković, N.; Jovanović, D.; Veljković, S.; Randjelović, B.; Vlahović, B. Fractal frontiers in microelectronic ceramic materials. *Ceram. Int.* **2019**, *45*, 9679–9685. [CrossRef]
31. Mitic, V.V.; Lazovic, G.; Mirjanic, D.; Fecht, H.; Vlahovic, B.; Arnold, W. The fractal nature as new frontier in microstructural characterization and relativization of scale sizes within space. *Mod. Phys. Lett. B* **2020**, *34*, 2050421. [CrossRef]
32. Mitic, V.V.; Kostic, L.j.; Paunovic, V.; Lazovic, G.; Miljkovic, M. Fractal nature structure reconstruction method in designing microstructure properties. *Mater. Res. Bull.* **2018**, *101*, 175–183. [CrossRef]
33. Taylor, R.P.; Spehar, B. Fractal Fluency: An intimate relationship between the brain and processing of fractal stimuli. In *The Fractal Geometry of the Brain*; Ieva, A.D., Ed.; Springer: New York, NY, USA, 2016; pp. 485–496.
34. Kenkel, N.C.; Walker, D.J. Fractals in the biological sciences. *Coenoses* **1996**, *11*, 77–100.
35. Dimri, V.P. *Application of Fractals in Earth Sciences*; CRC Press: Rotterdam, The Netherlands, 2000.
36. Lanza, L.G.; Gallant, J. Fractals and Similarity Approaches in Hydrology. In *Encyclopedia of Hydrological Sciences*; Anderson, M.G., Ed.; John Wiley and Sons: New York, NY, USA, 2006.
37. Cohen, N. Fractal Antennas and Fractal Resonators. U.S. Patent 6452553B1, 9 August 1995.
38. Baliarda, C.P. Space-Filling Miniature Antennas. U.S. Patent 8207893B2, 19 January 2000.
39. Mitic, V.V.; Lazovic, G.; Lu, C.A.; Paunovic, V.; Radovic, I.; Stajcic, A.; Vlahovic, B. The nano-scale modified $BaTiO_3$ morphology influence on electronic properties and ceramics fractal nature frontiers. *Appl. Sci.* **2020**, *10*, 3485. [CrossRef]
40. Kozlov, G.V.; Dolbin, I.V. Effect of a nanofiller structure on the degree of reinforcement of polymer–carbon nanotube nanocomposites with the use of a percolation model. *J. Appl. Mech. Tech. Phys.* **2018**, *59*, 765–769. [CrossRef]
41. Ţălu, Ş.; Abdolghaderi, S.; Pinto, E.P.; Matos, R.S.; Salerno, M. Advanced fractal analysis of nanoscale topography of Ag/DLC composite synthesized by RF-PECVD. *Surf. Eng.* **2020**, *36*, 713–719. [CrossRef]
42. Amâncio, M.A.; Pinto, E.P.; Matos, R.S.; Nobre, F.X.; Brito, W.R.; da Fonseca Filho, H.D. Nanoscale morphology and fractal analysis of TiO2 coatings on ITO substrate by electrodeposition. *J. Microsc.* **2021**, *282*, 162–174. [CrossRef] [PubMed]
43. Xie, N.; Shao, W.; Feng, L.; Lv, L.; Zhen, L. Fractal Analysis of Disordered Conductor–Insulator Composites with Different Conductor Backbone Structures near Percolation Threshold. *J. Phys. Chem. C* **2012**, *116*, 19517–19525. [CrossRef]
44. Pramanik, B.; Tadepalli, T.; Mantena, P.R. Surface Fractal Analysis for Estimating the Fracture Energy Absorption of Nanoparticle Reinforced Composites. *Materials* **2012**, *5*, 922–936. [CrossRef] [PubMed]
45. Qiang, T.; Yu, D. Correlation between Fractal Dimension and Impact Strength for Wood Plastic Composites. *Adv. Mater. Res.* **2012**, *411*, 548–551. [CrossRef]
46. Yang, Y.; Cheng, H.; Liang, B.; Hou, G.; Zhao, D.; Liu, C.; Zhang, K. Fractal characteristic evaluation and interpolation reconstruction for surface topography of drilled composite hole wall. *Front. Mech. Eng.* **2021**, *16*, 840–854. [CrossRef]
47. Gusev, B.; Grishina, A.; Korolev, E.; Ayzenshtadt, A. Strength equation of composite materials and fractal dimension of cracks. *Energy Rep.* **2021**, *7*, 569–578. [CrossRef]
48. Xia, D.; Chen, R.; Zhang, D.; Cheng, J. Relationship between Fractal Dimension and Properties of Engineered Cementitious Composites with Different Aggregates. *Materials* **2022**, *15*, 7666. [CrossRef]
49. Eyssautier, J.; Levitz, P.; Espinat, D.; Jestin, J.; Gummel, J.; Grillo, I.; Barré, L. Insight into Asphaltene Nanoaggregate Structure Inferred by Small Angle Neutron and X-ray Scattering. *J. Phys. Chem. B* **2011**, *115*, 6827–6837. [CrossRef]
50. Buescu, J.; Serpa, C. Fractal and Fractal dimensions for systems of iterative functional equations. *J. Math. Anal. Appl.* **2019**, *480*, 123429. [CrossRef]
51. Serpa, C.; Buescu, J. Constructive Solutions for Systems of Iterative Functional Equations. *Constr. Approx.* **2017**, *45*, 273–299. [CrossRef]
52. Serpa, C. Affine Fractal Least Squares Regression Model. *Fractals* **2022**, *30*, 2250138. [CrossRef]
53. Barnsley, M.F. Fractal functions and interpolation. *Constr. Approx.* **1986**, *2*, 303–329. [CrossRef]